The Journal of Immunology

Immunoproteasomes Down-Regulate Presentation of a Subdominant T Cell Epitope from Lymphocytic Choriomeningitis Virus

Michael Basler, Nikolay Youhnovski, Maries van den Broek, Michael Przybylski and Marcus Groettrup

J Immunol 2004; 173:3925-3934; ;
doi: 10.4049/jimmunol.173.6.3925
http://www.jimmunol.org/content/173/6/3925

The Journal of Immunology is published twice each month by
The American Association of Immunologists, Inc.,
1451 Rockville Pike, Suite 650, Rockville, MD 20852

Print ISSN: 0022-1767 Online ISSN: 1550-6606.

Immunoproteasomes Down-Regulate Presentation of a Subdominant T Cell Epitope from Lymphocytic Choriomeningitis Virus[1]

Michael Basler,* Nikolay Youhnovski,† Maries van den Broek,‡ Michael Przybylski,† and Marcus Groettrup[2]*

The cytotoxic T cell response to pathogens is usually directed against a few immunodominant epitopes, while other potential epitopes are either subdominant or not used at all. In C57BL/6 mice, the acute cytotoxic T cell response against lymphocytic choriomeningitis virus is directed against immunodominant epitopes derived from the glycoprotein (gp33–41) and the nucleoprotein (NP396–404), while the gp276–286 epitope remains subdominant. Despite extensive investigations, the reason for this hierarchy between epitopes is not clear. In this study, we show that the treatment of cells with IFN-γ enhanced the presentation of gp33–41, whereas presentation of the gp276–286 epitope from the same glycoprotein was markedly reduced. Because proteasomes are crucially involved in epitope generation and because IFN-γ treatment in vitro and lymphocytic choriomeningitis virus infection in vivo lead to a gradual replacement of constitutive proteasomes by immunoproteasomes, we investigated the role of proteasome composition on epitope hierarchy. Overexpression of the active site subunits of immunoproteasomes LMP2, LMP7, and MECL-1 as well as overexpression of LMP2 alone suppressed the presentation of the gp276–286 epitope. The ability to generate gp276–286-specific CTLs was enhanced in LMP2- and LMP7-deficient mice, and macrophages from these mice showed an elevated presentation of this epitope. In vitro digests demonstrated that fragmentation by immunoproteasomes, but not constitutive proteasomes led to a preferential destruction of the gp276 epitope. Taken together, we show that LMP2 and LMP7 can at least in part determine subdominance and shape the epitope hierarchy of CTL responses in vivo. ***The Journal of Immunology,*** **2004, 173: 3925–3934.**

Cytotoxic T lymphocytes recognize peptide epitopes presented on MHC class I molecules, which allows CTLs to monitor for cells harboring intracellular pathogens. CTL responses are usually directed against one or a few dominant epitopes and some minor epitopes. Several factors that contribute to this phenomenon of immunodominance have been described (1–4). Viral proteins have to be targeted for degradation at a sufficient frequency (5), and they must be fragmented into peptides that meet the requirements for binding to the TAP as well as to a given MHC class I molecule with respect to their length and the availability of anchor residues (6). CTLs need to be triggered by their nominal epitope in the context of the appropriate class I molecule for an extended period of time, which implies that the affinity of the peptide to the binding groove of class I should be high. In addition, an adequate avidity of the TCR for the class I/peptide complex is pivotal (7). Finally, the precursor frequence of T cells with a particular specificity will determine whether a given epitope achieves immunodominance over competing epitopes (3, 8).

The infection of the mouse with lymphocytic choriomeningitis virus (LCMV)[3] is a frequently used model of viral infection, and also, the phenomenon of immunodominance has been thoroughly investigated (2, 8, 9–12). In C57BL/6 mice, this response is dominated by CTLs specific for the H-2D^b-restricted epitopes gp33–41, nucleoprotein 396–404 (NP396–404), and the subdominant epitope gp276–286. The reasons for gp276 subdominance have been thoroughly investigated in the past (11). One contributing factor to the subdominance of gp276 could be that the amount of gp276 epitopes that was eluted from 10^9 LCMV-infected MC57 fibroblasts (0.16 ng) was about twice as low as that of NP396 (0.3 ng) and 12-fold lower than gp33 (2.0 ng). This amount corresponded to 92 H-2D^b-bound gp276 epitopes per MC57 cell, which is in a range in which it could become limiting for the recognition by gp276-specific CTLs (13, 14). It hence appears that the intracellular processing of gp276 is less efficient than processing of the gp33 epitope derived from the same glycoprotein. Because the proteasome is involved in the processing of both epitopes (15), we decided to further investigate its impact on the establishment of the epitope hierarchy.

The proteasome is the main protease in the cytoplasm and the nucleus that generates the C termini of most peptide ligands of MHC class I molecules (16, 17). The proteolytic core complex of the proteasome system is the 20S proteasome, which is constructed like a cylinder of four stacked rings. The outer two rings consist of seven different α-type subunits that bind to regulatory complexes of the 20S core particle, whereas the two inner rings are made up of seven different subunits of the β-type. Three of the β-subunits,

*Division of Immunology, Department of Biology, and †Laboratory of Analytical Chemistry, Department of Chemistry, University of Constance, Konstanz, Germany; and ‡Institute of Experimental Immunology, Department of Pathology, University Hospital Zürich, Zürich, Switzerland

Received for publication October 30, 2003. Accepted for publication July 2, 2004.

The costs of publication of this article were defrayed in part by the payment of page charges. This article must therefore be hereby marked *advertisement* in accordance with 18 U.S.C. Section 1734 solely to indicate this fact.

[1] This work was supported by grants of the Swiss National Science Foundation (31-52284.97/1) and the University of Constance to M.G., and by a grant from the Cloëtta Foundation, Zürich, to M.v.d.B.

[2] Address correspondence and reprint requests to Dr. Marcus Groettrup, Department of Biology, Division of Immunology, University of Constance, P1101 Universitätsstrasse 10, D-78457 Konstanz, Germany. E-mail address: Marcus.Groettrup@uni-konstanz.de

[3] Abbreviations used in this paper: LCMV, lymphocytic choriomeningitis virus; ESI-MS, electrospray ionization mass spectrometry; NP, nucleoprotein; VV, vaccinia virus.

0022-1767/04/$02.00

designated δ (β1), MB1 (β5), and MC14 (Z, β2), bear the active centers of the 20S proteasome. Upon stimulation of cells with the inflammatory cytokine IFN-γ, these constitutively expressed subunits are replaced by inducible subunits named LMP2 (β1i), LMP7 (β5i), and MECL-1 (β2i) during the de novo assembly of 20S proteasomes. This subunit exchange alters the cleavage pattern of the proteasome (16), which can lead to an enhancement of Ag presentation (18–21). However, for a few epitopes from human tumors, the induction of immunoproteasomes was found to negatively affect their presentation (22). Although gene-targeted mice deficient for LMP2 (23) and LMP7 (24) have been generated almost a decade ago, the impact of these two subunits on the hierarchy of epitopes has been barely investigated, except for a recent study by Chen et al. (25), which shows that in LMP2$^{-/-}$ mice the CTL response to influenza virus follows a different hierarchy than in wild-type mice. This effect was due both to differences in the CTL precursor frequency as well as to changes in epitope presentation.

Another IFN-γ-inducible complex, which affects epitope generation and therefore has the potential to shape epitope hierarchies, is the 11S regulator of the proteasome (26) (also called PA28 (27)). PA28 consists of two different subunits, α and β, which form a heptameric ring that binds to the 20S or 26S proteasomes and affects their peptidolytic properties (28). Overexpression of PA28αβ has been shown to enhance the presentation of a number of epitopes (29–32), and, conversely, PA28 deficiency in PA28β$^{-/-}$ or PA28αβ$^{-/-}$ mice interferes with epitope presentation in several cases (33, 34).

In this study, we investigated whether the composition of proteasome active site subunits and PA28 could be involved in determining immunodominance and subdominance in the LCMV system. The finding that the IFN-γ treatment of MC57 fibroblasts enhanced gp33 presentation, but down-regulated the presentation of gp276 inspired our work. With the help of transfectants and knockout mice, we could indeed show that immunoproteasomes negatively affect gp276 processing and presentation in vitro and the generation of gp276-specific CTLs in vivo. Our data are discussed with respect to so far elusive changes of epitope hierarchy in acute vs persistent LCMV infection and in relation to different Ag presentation by fibroblasts as opposed to dendritic cells.

Materials and Methods

Mice and viruses

C57BL/6 mice (H-2^b) were purchased from the animal facility of University of Constance. LMP2$^{-/-}$ (23) and LMP7$^{-/-}$ (24) gene-targeted mice were provided by J. Monaco (Department of Molecular Genetics, Cincinnati Medical Center, Cincinnati, OH), while PA28αβ mice were kindly contributed by T. Chiba (Department of Molecular Oncology, Tokyo Metropolitan Institute of Medical Science, Tokyo, Japan) (34). All knockout mice were backcrossed onto the C57BL/6 background for at least 10 generations. Mice were kept in a specific pathogen-free facility and used at 6–10 wk of age. LCMV-WE was originally obtained from F. Lehmann-Grube (Heinrich Pette Institut, Universität Hamburg, Hamburg, Germany) and propagated on the fibroblast line L929. Recombinant vaccinia virus (rVV) encoding the LCMV glycoprotein (rVVG2) was obtained from D. Bishop (Institute of Virology, Oxford, U.K.) and was propagated on BSC40 cells. Mice were infected with 200 PFU of LCMV-WE i.v. or with 2×10^6 PFU of VVG2 i.p., and the specific CTL response was analyzed at day 8 or 6 after infection, respectively.

Cell lines

MC57 (H-2^b) is a C57BL/6-derived methylcholanthrene-induced fibrosarcoma cell line (35). MCGP (H-2^b) is a MC57-derived transfectant expressing the LCMV glycoprotein. B8 is a BALB/c-derived fibroblast line (H-2^d) obtained by SV40 infection in vitro (28). B27M6 and B27M2 are triple transfectants of B8 cells expressing murine LMP2, LMP7, and MECL-1; BPαβ13 is a double transfectant of B8 cells expressing murine PA28α and PA28β (19); BC2P6 is a transfectant of B8 cells expressing murine LMP2 (28); B7H6 is a transfectant of B8 cells expressing murine LMP7 (28). Hyb33 and Hyb276 are T cell hybridomas specific for gp33–41/H-2K^b or gp276–286/H-2D^b, respectively (15). All cells were grown in IMDM supplemented with 2 mM glutamine, 10% FCS, and 100 U/ml penicillin/streptomycin. Selection drugs were required for MCGP (0.8 mg/ml G418), B27M6Db (0.5 mg/ml G418, 3 μg/ml puromycin, 0.4 mg/ml hygromycin B, 5 μg/ml blasticidin), BPαβ13Db (0.5 mg/ml G418, 3 μg/ml puromycin, 0.4 mg/ml hygromycin B, 5 μg/ml blasticidin), B8Db (5 μg/ml blasticidin), B7H6Db and BC2P6Db (3 μg/ml puromycin, 0.4 mg/ml hygromycin B), and Hyb33 and Hyb276 (1× hypoxanthine thymidine, 0.5 mg/ml hygromycin B).

Synthetic peptides

The synthetic peptides gp33–41 (KAVYNFATC) and gp276–286 (SGVENPGGYCL) were obtained from Echaz Microcollections (Tubingen, Germany). The 25-mer peptide used for proteasome digestion encompassing LCMV-glycoprotein residues 271–295 (TLSSDSSGVEDPG GYCLTKWMILAAE) was synthesized by solid-phase peptide synthesis on a NovaSyn TGA resin (0.21 mmol/g) by Fmoc/tBu chemistry, using a semiautomated Economy Peptide Synthesizer EPS-221 (Abimed, Germany). The crude peptide was purified by reverse-phase HPLC on a C18 column (GROM-SIL 120 ODS-4 HE, 10 μm, 250 × 20 mm; Grom, Herrenberg-Kayh, Germany) using as mobile phases: eluent A (0.1% trifluoroacetic acid in water) and eluent B (80% AcCN, 0.1% trifluoroacetic acid in water). The following gradient was applied: 0 min, 10% eluent B; 45 min, 90% eluent B.

Antibodies

KL 25 is a mouse mAb reactive with the LCMV glycoprotein (36). The mAb KH95 (BD Pharmingen, San Diego, CA) reacts with the H-2D^b MHC class I molecule.

Flow cytometry

A number of 5×10^5 infected and noninfected B8Db, B27M6Db, B27M2Db, B7H6Db, BC2P6Db, and BPαβ13Db cells in 100 μl of PBS + 2% FCS were incubated in a round-bottom 96-well plate on ice for 20 min with 1 μg of mAb KL25, washed twice, and subsequently stained by a FITC-conjugated sheep anti-mouse Ig (Silenus, Victoria, Australia) for another 20 min on ice. Samples were washed twice and analyzed on a FACScan flow cytometer (BD Biosciences, Mountain View, CA). To check transfected B8Db, B27M6Db, B27M2Db, B7H6Db, BC2P6Db, and BPαβ13Db for H-2D^b expression, the staining was performed, as described above, with the H-2D^b-specific Ab KH95.

For Vβ staining splenocytes from uninfected or LCMV (8 days postinfection with 200 PFU of LCMV-WE i.v.)-infected C57BL/6, LMP2$^{-/-}$, and LMP7$^{-/-}$ mice were treated with 1.66% NH_4Cl (w/v), washed twice, and incubated for 30 min with biotin-conjugated anti-Vβ8.1/8.2, anti-Vβ9, or anti-Vβ10b (BD Pharmingen) Abs on ice. Samples were washed twice and incubated for another 30 min with streptavidin-conjugated FITC and Cy5-conjugated mouse anti-CD8 (BD Pharmingen). After two washes, cells were acquired with the use of FACScan flow cytometer (BD Biosciences, Mountain View, CA) and analyzed with the FlowJo software (Tree Star, San Carlos, CA). Differences between groups were assessed by unpaired *t* test (www.graphpad.com). Values of $p < 0.05$ are considered to be statistically significant.

Transfections

B8, B27M6, and BPαβ13 were transfected with an expression plasmid encoding H-2D^b (a kind gift from F. Momburg, Heidelberg, Germany). Cells were plated to 80% confluence and were transfected by the standard calcium phosphate coprecipitation method with 10 μg of H-2D^b plasmid and 2 μg of blasticidin resistance vector pcDNA6/TR (Invitrogen Life Technologies, Karlsruhe, Germany). Two days after transfection, cells were plated in 96-well plates under cloning conditions and selected with 5 μg/ml blasticidin (Invitrogen Life Technologies). Because of instability of blasticidin, the selection medium was replaced every 4 days. Blasticidin-resistant cells were tested for H-2D^b expression by FACS analysis, and positive cells were subcloned to obtain monoclonal cells.

B27M2, BC2P6, and B7H6 cells were stably transfected with H-2D^b plasmid and either hygromycin or puromycin resistance plasmids, according to the manufacturer's protocol (FuGENE 6; Roche, Basel, Switzerland). Clonal and selection drug-resistant cells were tested for H-2D^b expression by flow cytometry.

LacZ assay

For the lacZ assay, 5×10^4 LCMVgp33–41/H-2K^b- or LCMVgp276–286/H-2D^b-specific T cell hybridomas (15) were cocultured overnight with

2.5×10^4 stimulator cells in 96-well plates. As stimulator cells, MCGP, B8Db, B27M6Db, B27M2Db, BC2P6Db, B7H6Db, and PB$\alpha\beta$13Db, or thioglycolate-elicited peritoneal macrophages from C57BL/6, LMP2$^{-/-}$, or LMP7$^{-/-}$ mice were used. MCGP cells were treated for 3 days with 60 U/ml murine rIFN-γ (Roche) to allow a complete replacement of constitutive proteasomes by immunoproteasomes (19). The lacZ-based color reaction was performed and measured, as detailed elsewhere (15).

Restimulation and cytolytic assay

B6, LMP2$^{-/-}$, and LMP7$^{-/-}$ mice were infected with 2×10^6 VVG2 i.p. Six days later, 4×10^6 splenocytes were cocultured with 2×10^6 peptide-loaded (gp33–41 or gp276–286) irradiated (2000 rad) syngeneic splenocytes in 2 ml of IMDM supplemented with 10% FCS, penicillin/streptomycin, 2-ME, and 10% Con A supernatant (Con A-induced rat spleen culture supernatant) in 24-well plates. After 6 days of culture, a standard ^{51}Cr release assay with peptide (gp33–41 or gp276–286)-loaded (10^{-6} M) or unloaded MC57 cells was performed. In brief, target cells were incubated with $Na_2{}^{51}CrO_4 \pm$ peptide for 90 min. Three-fold dilutions of the restimulated cultures were tested for cytotoxic activity using 10^4 ^{51}Cr-labeled MC57 as targets in a 5-h chromium release assay. The percentage of specific lysis was calculated as follows: percentage of specific release = (experimental release –spontaneous release) ÷ (maximal release –spontaneous release) × 100%. The spontaneous lysis was below 15%; the lysis of unloaded targets was below 10%.

Intracellular staining for IFN-γ

A total of 2×10^6 splenocytes was incubated in round-bottom 96-well plates with 10^{-7} M of the specific peptide in 100 μl of 10% IMDM for 2 h at 37°C. Then brefeldin A (10 μg/ml) was added, and the incubation was continued for another 4 h. Cells were incubated for 20 min at 4°C with Cy5-conjugated mouse anti-CD8 (clone 53-6.7; BD Pharmingen). Following fixation with 4% paraformaldehyde at 4°C for 5 min, the cells were incubated overnight with fluorescein-conjugated mouse anti-IFN-γ (clone XMG1.2; BD Pharmingen) in PBS containing 2% FCS and 0.1% (w/v) saponin (Sigma-Aldrich, St. Louis, MO). Samples were washed twice, acquired with the use of FACScan flow cytometer (BD Biosciences), and analyzed by the FlowJo software (Tree Star).

Metabolic labeling, immunoprecipitation, and two-dimensional gel electrophoresis

A total of 10^7 thioglycolate-elicited peritoneal macrophages from BALB/c mice was starved in cysteine/methionine-free RPMI 1640, 10% dialyzed FCS for 1 h at 37°C and labeled with 0.2 mCi/ml Met-[^{35}S]-label (Hartmann Analytic, Braunschweig, Germany) for 8 h to allow full maturation of the proteasome. Cells were washed with PBS, harvested, and lysed for 30 min on ice in 20 mM Tris/HCl, pH 7.5, 150 mM NaCl, 1 mM $MgCl_2$, and 2% Triton X-100. The lysate was precleared for 1 h with protein A-Sepharose CL-4B (Amersham Biosciences, Uppsala, Sweden), followed by overnight immunoprecipitation with an antiproteasome serum bound to protein A-Sepharose at 4°C. The precipitates were washed four times with NET-TON (650 mM NaCl, 5 mM EDTA, 50 mM Tris-HCl, 0.5% Triton-X-100, 0.05% NaN_3, 1 mg/ml OVA) and twice with NET-T (150 mM NaCl, 5 mM EDTA, 50 mM Tris-HCl, 0.5% Triton X-100, 0.05% NaN_3), and separated by nonequilibrium pH-gradient gel electrophoresis/SDS-PAGE, as previously described (28), and visualized by autoradiography on a Fuji BAS1500 radioimager.

Purification of 20S proteasome

The lysis of organ tissue, the purificaton of 20S proteasomes from liver, and the quantification of the 20S proteasome from uninfected and LCMV-infected (8 days postinfection with 200 PFU of LCMV-WE i.v.) C57BL/6, LMP2$^{-/-}$, and LMP7$^{-/-}$ mouse livers were performed, as previously described (28).

Proteasomal fragmentation of polypeptide and mass spectrometric analysis of peptide products

Digestions of the 25-mer polypeptide spanning LCMV-WE glycoprotein residues 271–295 with purified 20S proteasomes were performed for indicated time periods exactly as previously described (19). HPLC-electrospray ionization mass spectrometry (ESI-MS) analysis was performed on a Q-Trap mass spectrometer (Applied Biosystems, Concord, Canada) equipped with Turbospray Ion Source (Applied Biosystems) and Agilent (Palo Alto, CA) 1100 HPLC system (Autosampler G1313A, Binary Pump G1312A, on-line vacuum degasser G1322A), ACCURATE flow splitter AC-100-VAR with 0.3 mm I.D. splitter capillary CAL-100-0.3 (LC Packings, Amsterdam, Holland), and control software: Analyst 1.3.2 (Applied Biosystems) under Windows 2000 operating system. HPLC conditions: mobile phase solvent A 0.1% aqueous solution of HCOOH, solvent B 0.1% solution of HCOOH in acetonitrile with following gradient: 0 min, 0% B; 4 min, 0% B; 44 min, 80% B. Binary pump flow 100 μl/min and after splitting (on column) 4–10 μl/min. The HPLC column was PepMap C18, 3 μm, 100 Å, 300 μm I.D. × 5 cm (LC Packings). MS conditions: scan type: enhanced MS; positive mode; mass range 340-1400 amu; declustering potential 30 V; entrance potential 10 V; curtain gas 20 PSI; ion source gas 1: 15 PSI; ion spray voltage 5000 V; source temperature 200°C. Sample injection volume 1 μl.

Results

Effect of IFN-γ on the presentation of gp33–41 and gp276–286

The stimulation of cells with IFN-γ strongly induces many proteins along the MHC class I presentation pathway, thus leading to a marked up-regulation of class I cell surface expression (16). When we infected the C57BL/6-derived mouse fibroblast line MC57 with the LCMV strain WE and treated the cells with or without murine IFN-γ for 3 days, we observed that IFN-γ caused a 2- to 3-fold up-regulation in the presentation of the immunodominant epitope gp33 as determined with a gp33-specific T cell hybridoma in a lacZ-based colorigenic assay (37) (Fig. 1*A*). Despite a ~10-fold increase of bulk H-2D^b and H-2K^b class I cell surface expression (data not shown), the presentation of the subdominant gp276 epitope was consistently down-regulated by IFN-γ treatment by a factor of ~2 in the same assay. Although we confirmed that the cells were equally infected with LCMV by determining the cell surface expression of the LCMV glycoprotein by flow cytometry (data not shown), we wanted to rule out that the obtained result is linked to IFN-γ-dependent changes in viral replication and Ag production. We hence repeated this experiment with the MCGP line, which is a stable MC57 transfectant expressing the LCMV glycoprotein. Also in this virus-independent model, we observed an IFN-γ-dependent up-regulation of gp33 presentation, whereas presentation of the gp276 epitope was markedly reduced (Fig. 1*B*).

Effect of the immunoproteasome subunits LMP2, LMP7, and MECL-1 as well as PA28$\alpha\beta$ on the presentation of gp276–286

Numerous gene products are induced with IFN-γ, which could account for an enhancement of gp33 presentation, but only few candidates are known that could be responsible for the down-regulation of gp276 presentation. Given that immunoproteasomes have been shown to interfere with the presentation of some tumor epitopes (22), we examined whether the IFN-γ-inducible proteasome subunits LMP2, LMP7, and MECL-1, or the IFN-γ-inducible proteasome activator PA28$\alpha\beta$ could mediate the observed down-regulation of gp276 presentation. Previously, we have generated and carefully characterized stable transfectants of the mouse fibroblast line B8, which coexpress either all three active site subunits of immunoproteasomes (designated B27M6 or B27M2) or the α- and β-subunits of the proteasome regulator PA28$\alpha\beta$ (designated BP$\alpha\beta$13) to the same degree as B8 fibroblasts after 3 days of IFN-γ treatment (19). Because the recipient line B8 is derived from a BALB/c mouse (H-2^d), we supertransfected the recipient line B8 as well as B27M6 and BP$\alpha\beta$13 cells with an expression construct encoding the H-2D^b restriction element. Clones named B8Db, B27M6Db, B27M2Db, and BP$\alpha\beta$13Db, respectively, were selected that, according to flow cytometry, expressed similar levels of H-2D^b class I molecules on the cell surface (Fig. 2*B*). Interestingly, when these clones were infected for 1.5 days with LCMV-WE and examined for gp276 presentation with our gp276/H-2D^b-specific hybridoma, we found that the combined overexpression of LMP2, LMP7, and MECL-1 in B27M6Db and B27M2Db cells reduced gp276 presentation 2- to 3-fold compared

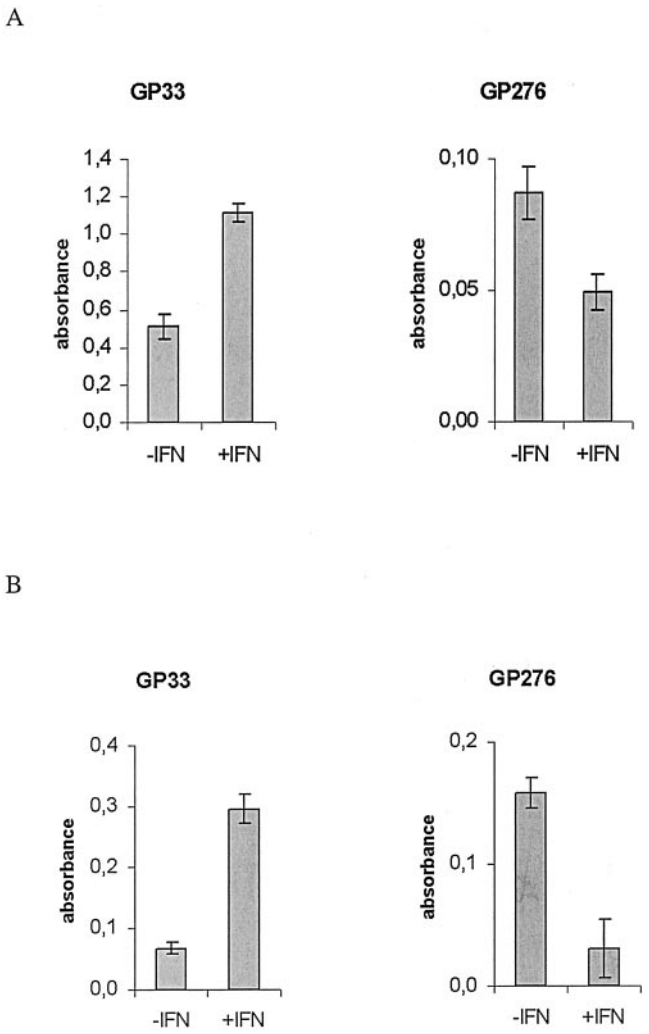

FIGURE 1. Comparison of the presentation of the LCMV epitopes gp33 and gp276 in ±IFN-γ-treated and LCMV-infected MC57 cells (*A*) and the LCMV glycoprotein transfectant MCGP (*B*). Stimulator cells were treated for 3 days with 60 U/ml IFN-γ or left untreated, and LCMV infection was performed in vitro a few hours before initiation of IFN-γ treatment. The stimulation of gp33- and gp276-specific T cell hybridomas was determined in chromogenic lacZ assays. The *y*-axis shows absorbance of enzymatically converted chromogen at 570 nm in lacZ assays. The values are means of three replicate cultures; shown is a representative experiment of three experiments that yielded similar results. Error bars represent SDs.

with B8Db cells, whereas PA28$\alpha\beta$ overexpression had only a minor effect (Fig. 2, *A* and *C*). This result, which was confirmed with independent clones, strongly suggested that the induction of immunoproteasomes is at least in part responsible for the IFN-γ-mediated down-regulation of gp276.

To investigate the effect of LMP2 only and LMP7 only, we stably supertransfected the well-characterized cell lines BC2P6 (B8 cell-overexpressing LMP2) and B7H6 (B8 cell-overexpressing LMP7) (28) with an expression construct encoding the H-2D^b restriction element (Fig. 2, *C* and *D*). These clones were infected with LCMV, and the presentation of gp276 was examined with gp276/H-2D^b-specific hybridomas. Cells overexpressing LMP7 showed no altered presentation of gp276 compared with the parental cells (Fig. 2*C*). In contrast, LMP2 overexpression reduced gp276 presentation ~4-fold, which indicates that the reduced presentation of gp276 in LMP2/LMP7/MECL-1 cells (Fig. 2, *A* and *C*) is mainly due to LMP2.

Comparison of gp33 and gp276 presentation by LCMV-infected macrophages from C57BL/6, LMP2$^{-/-}$, and LMP7$^{-/-}$ mice

To confirm this effect of immunoproteasomes in an independent system and to discriminate whether LMP2 or LMP7 contributes to down-regulation of gp276 presentation, we examined Ag presentation by LCMV-infected thioglycolate-elicited peritoneal macrophages from LMP2$^{-/-}$ and LMP7$^{-/-}$ gene-targeted as well as C57BL/6 control mice. The peritoneal macrophages were infected in vitro for 20 h with LCMV-WE and analyzed for gp33 and gp276 presentation with the respective T cell hybridomas (Fig. 3) using peptide-pulsed MC57 cells as specificity controls (*lanes 1* and *2*) and uninfected peritoneal macrophages from C57BL/6, LMP2$^{-/-}$, and LMP7$^{-/-}$ mice as negative controls (*lanes 3–5*). Although no difference in gp33 presentation was found between C57BL/6 and LMP2$^{-/-}$ macrophages, gp33 presentation was reduced by ~50% in LCMV-WE-infected macrophages from LMP7$^{-/-}$ mice. This result suggests that the induction of LMP7, but not of LMP2, contributes to the IFN-γ-dependent enhancement of gp33 presentation (Fig. 1*A*). The presentation of gp276, in contrast, seems to benefit from the deficiency of LMP7 and to a minor extent from LMP2 as macrophages from the respective knockout mice stimulated gp276-specific hybridomas better than macrophages from the wild-type control. This result is consistent with the aforementioned reduction in gp276 presentation caused by immunoproteasome overexpression (Fig. 2*B*).

To address to which extent LMP2 and LMP7 are expressed in thioglycolate-elicited peritoneal macrophages, these cells were metabolically labeled with [^{35}S]Met/Cys. The proteasomes were immunoprecipitated and the subunit composition was analyzed by nonequilibrium pH-gradient gel electrophoresis/SDS-PAGE. LMP7 (bearing 15 Met/Cys in the primary structure) was prominently expressed in thioglycolate-elicited peritoneal macrophages, as evidenced by the intensity of the LMP7 spots, and the virtually complete replacement of the homologous subunit MB-1 (bearing 9 Met/Cys). LMP2 (bearing 8 Met/Cys), in contrast, was expressed to a lesser extent according to the low spot intensity and the prevalence of its constitutive homologue δ (containing 11 Cys/Met) (Fig. 3*B*). This might explain the only minor effect of LMP2 deficiency on gp276 presentation by peritoneal macrophages.

The generation of gp276-specific CTLs is improved in LMP2$^{-/-}$ and LMP7$^{-/-}$ mice

To investigate how LMP2 and LMP7 would affect the CTL response to gp33, gp276, and NP396 in vivo, we first infected LMP2$^{-/-}$, LMP7$^{-/-}$, and PA28$\alpha\beta^{-/-}$ knockout as well as C57BL/6 control mice with LCMV. However, standard ^{51}Cr release assays performed on day 8 postinfection with peptide-loaded target cells did not detect significant differences between these mice strains irrespective of whether we infected with LCMV-WE or LCMV-Armstrong (data not shown). Moreover, virus titers in the spleen obtained on day 4 postinfection were not different in control and knockout mice (Table I). These results are not unexpected given that LCMV replicates very fast in numerous mouse tissues to high titers and overwhelms the organism with viral Ags. Hence, we turned to infection of these mice with rVVG2. VV replicates much slower in mice, and therefore produces a lower amount of Ag. Splenocytes from rVVG2-infected mice were harvested on day 6 after infection, and the CTLs were restimulated in vitro for another 6 days before they were used as effectors in a chromium release assay. As shown in Fig. 4*A*, the lysis of targets loaded with the gp276 peptide by LMP2$^{-/-}$ and LMP7$^{-/-}$ effectors was much higher (40–75%) as compared with CTLs from C57BL/6 mice (15–25%). This indicates that, in agreement with

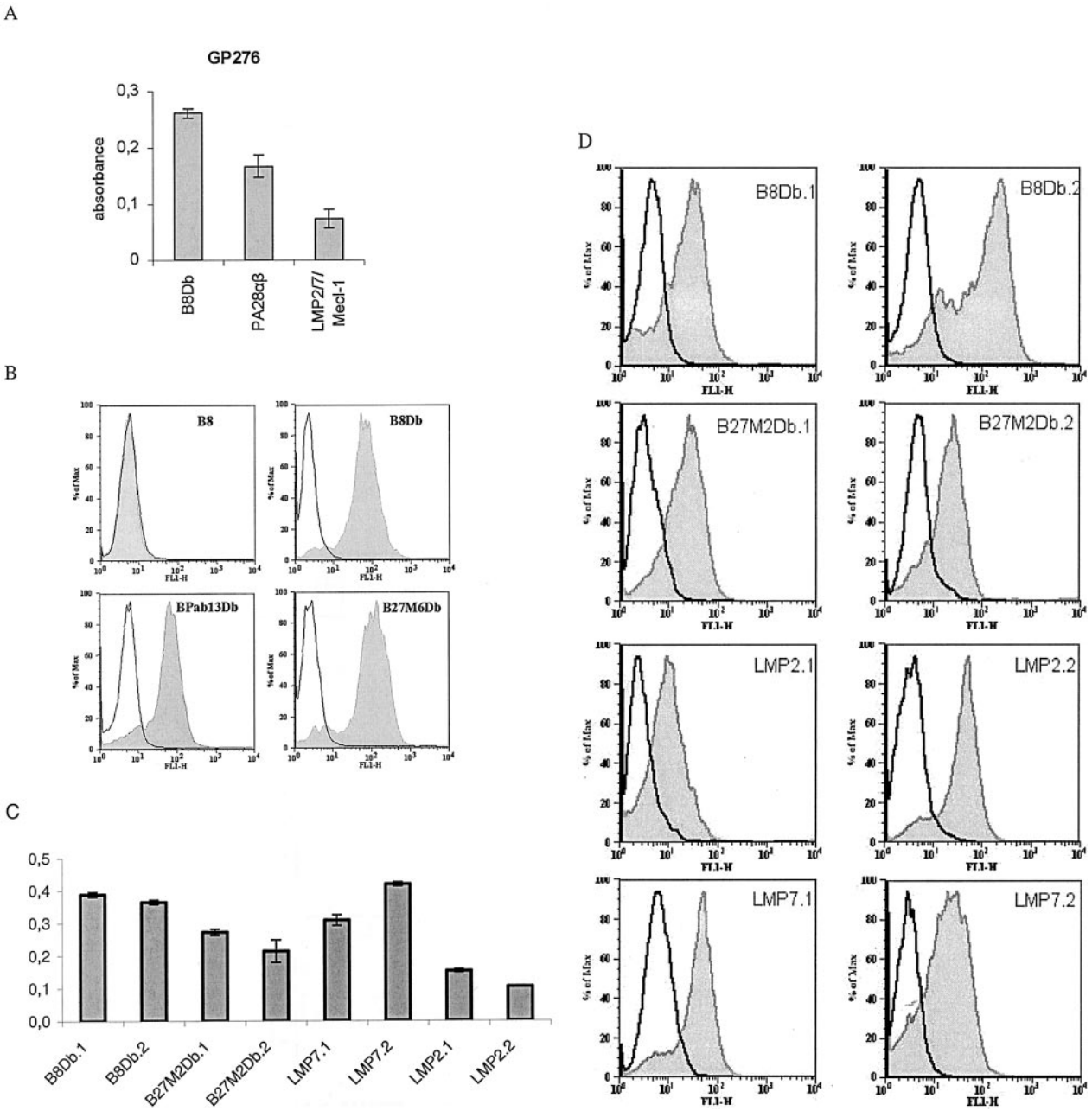

FIGURE 2. *A*, Comparison of the presentation of the LCMV-GP276 epitope by stable cell lines transfected with expression constructs for the restriction element H-2D^b as well as LMP2/LMP7/MECL-1 (B27M6Db) or PA28α and β (BP$\alpha\beta$13Db); B8Db are recipient cells only transfected for H-2D^b. The stimulator cells were infected with LCMV-WE in vitro 24 h before incubation with the gp276-specific hybridoma. The *y*-axis represents absorbance of enzymatically converted chromogen at 570 nm in lacZ assays. The values are the means of three replicate cultures; shown is a representative experiment of three experiments with similar outcome. Error bars represent SDs. *B* and *D*, To verify that H-2D^b cell surface expression was roughly equivalent in the different transfectants, a flow cytometric analysis was performed before every assay. *C*, Comparision of the presentation of gp276 epitope by stable cell lines transfected with H-2D^b (B8Db) as well as LMP2/LMP7/MECL-1 (B27M2Db), LMP7, or LMP2. The stimulator cells were infected with LCMV-WE in vitro 24 h before incubation with the gp276-specific hybridoma. The *y*-axis represents absorbance of enzymatically converted chromogen at 570 nm in lacZ assays. Two independent clones are shown for each transfection construct. The values are the means of three replicate cultures; shown is a representative experiment of three experiments with similar outcome. Error bars represent SDs.

our in vitro data, the gp276 epitope became immunodominant in the absence of either LMP2 or LMP7. The lysis of gp33-loaded targets varied between 20 and 40% for all mice, thus indicating that the replacement of constitutive proteasomes by immunoproteasomes did not significantly affect the generation of gp33-specific CTLs. Even with this more sensitive in vivo system, we failed to detect any differences between PA28$\alpha\beta^{-/-}$ and C57BL/6 wild-type mice with respect to the generation of either gp33- or gp276-specific CTLs (data not shown).

To confirm the observed enhancement in the generation of gp276-specific CTLs in LMP2- and LMP7-deficient mice, we performed double stainings of splenocytes from LMP2$^{-/-}$, LMP7$^{-/-}$, and C57BL/6 control mice for CD8 on the cell surface and for the intracellular content of IFN-γ (intracellular cytokine staining) on day 7 after infection with rVVG2. Also with this ex vivo assay, we observed that the generation of gp276-specific precursors was clearly enhanced in LMP2$^{-/-}$ and LMP7$^{-/-}$ mice (Fig. 4, *B* and *C*). In contrast, there was no difference in the

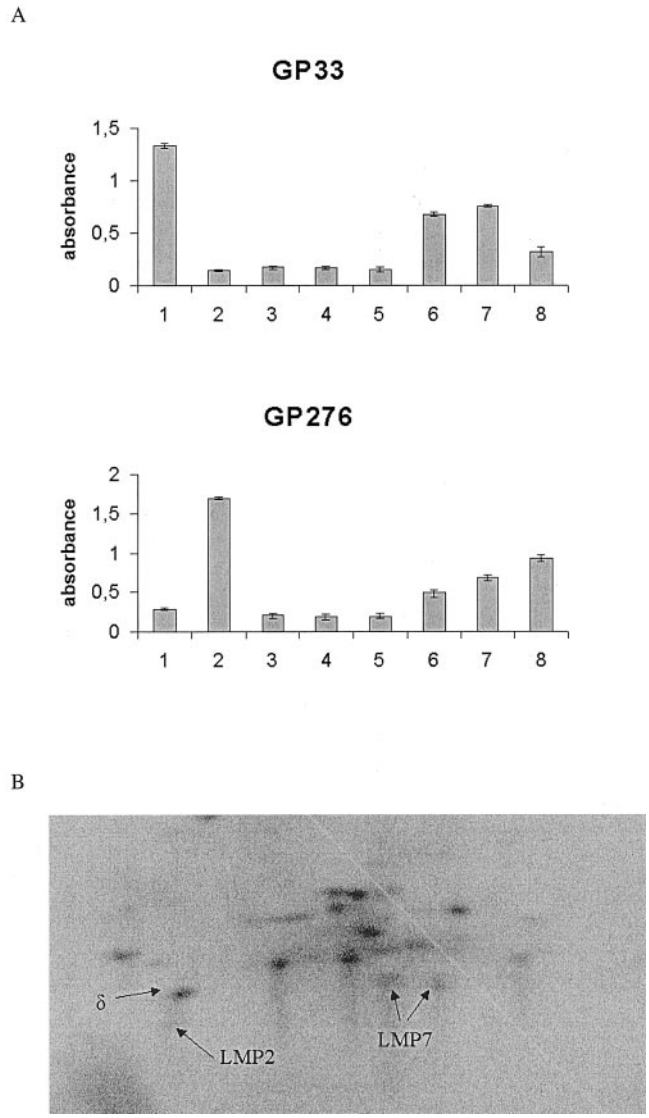

FIGURE 3. *A*, Presentation of gp33–41 and LCMV-gp276–286 epitopes by LCMV-infected macrophages from C57BL/6, LMP2$^{-/-}$, and LMP7$^{-/-}$ mice. Peritoneal macrophages were infected with LCMV-WE in vitro 1 day before addition of T cell hybridomas specific for gp33 (*upper panel*) or gp276 (*lower panel*); peptide-loaded MC57 cells served as specificity controls. The *y*-axis shows absorbance of enzymatically converted chromogen at 570 nm in lacZ assays. The values are the means of three replicate cultures. Error bars represent SDs. *Lane 1*, gp33-pulsed MC57; *lane 2*, gp276-pulsed MC57; *lane 3*, uninfected C57BL/6 macrophages; *lane 4*, uninfected LMP2$^{-/-}$ macrophages; *lane 5*, uninfected LMP7$^{-/-}$ macrophages; *lane 6*, infected C57BL/6 macrophages; *lane 7*, infected LMP2$^{-/-}$ macrophages; *lane 8*, infected LMP7$^{-/-}$ macrophages. The experiment has been repeated twice, giving similar results. *B*, Subunit composition of proteasomes from thioglycolate-elicited peritoneal macrophages. Thioglycolate-elicited peritoneal macrophages were metabolically labeled with [^{35}S]methionine/cysteine. Proteasomes were immunoprecipitated and analyzed for subunit composition on two-dimensional gels by autoradiography. LMP7, LMP2, as well as its constitutive homologue δ are labeled.

generation of gp33-specific CTLs in LMP2- and LMP7-deficient mice, compared with wild-type C57BL/6 mice (Fig. 4*B*). Taken together, it appears that the down-regulation of gp276 epitope presentation through LMP2 and LMP7 in vitro nicely correlates with an enhanced CTL elicitation in the respective gene-targeted mice.

Table I. *LCMV titers in spleen samples from C57BL/6, LMP2$^{-/-}$, and LMP7$^{-/-}$ mice 4 days after infection with 200 PFU of LCMV-WE*[a]

Mouse Strain	LCMV Titer
C57BL/6	$4.0 \pm 0.9 \times 10^5$
LMP2$^{-/-}$	$3.9 \pm 0.9 \times 10^5$
LMP7$^{-/-}$	$7.0 \pm 2.6 \times 10^5$

[a] Titers are given in PFU LCMV-WE per spleen.

The generation of Vβ10b-specific CTLs is impaired in LCMV-infected LMP2- and LMP7-deficient mice

To investigate whether the improved generation of gp276-specific CTLs in LMP2- and LMP7-deficient mice is due to an altered CTL repertoire, splenocytes from naive and LCMV-WE-infected (8 days postinfection with 200 PFU of LCMV-WE) C57BL/6, LMP2$^{-/-}$, and LMP7$^{-/-}$ mice were stained with different TCR-Vβ-specific Abs (Fig. 5). There was a significant difference (2% less) of Vβ8.1/8.2-specific CD8-positive cells in naive LMP2-deficient mice compared with C57BL/6 and LMP7-deficient mice. After LCMV infection, no difference could be detected for Vβ8. Naive LMP7$^{-/-}$ mice showed a slight, but significant difference for Vβ9-specific CTLs, which was abolished after LCMV infection. It has been shown that T cell lines specific for gp276 were using exclusively the Vβ10 variable segment for their TCRs (38). Naive LMP2$^{-/-}$ and LMP7$^{-/-}$ mice showed no difference in Vβ10 usage compared with C57BL/6. In contrast, after LCMV infection, the extent of CTLs using Vβ10 was significantly increased in C57BL/6 mice compared with LMP2- and LMP7-deficient mice.

In vitro fragmentation of the gp271–295 polypeptide by immunoproteasomes and constitutive proteasomes as well as LMP2- and LMP7-deficient proteasomes

Given that the generation of the gp276 epitope is dependent on proteasome activity (19), we hypothesized that gp276 presentation is adversely affected by LMP2 and LMP7 because constitutive proteasomes and immunoproteasomes fragment precursor polypeptides of gp276 in a different way. To test this hypothesis, we investigated how immunoproteasomes and constitutive 20S proteasomes fragment the 25-mer precursor polypeptide covering residues 271–295 of the LCMV-WE glycoprotein (NH_2-TLSDSSGVEDPGGYCLTKWMILAAE-COOH), which contains the underlined 11-meric gp276–286 epitope bearing an aspartate in position 5, which resulted from rapid deamidation of asparagine after systhesis (Fig. 6*A*). We isolated 20S proteasomes from the liver of uninfected mice as a source of constitutive proteasomes. Immunoproteasomes were isolated from the liver of mice on day 8 after LCMV infection. The subunit composition of the two proteasome populations on two-dimensional gels confirmed our previous finding that LCMV infection results in a virtually complete replacement of constitutive proteasomes by immunoproteasomes in vivo (39) (data not shown). The separation of the produced fragments after 8 h of in vitro digest by HPLC shows that constitutive proteasomes and immunoproteasomes fragment the 25-mer polypeptide in a different manner, and these differences in the HPLC profiles were confirmed in several independent experiments (Fig. 6*B*). The fragmentation was not observed in the presence of the proteasome inhibitor lactacystin, suggesting that 20S proteasomes were not contaminated by other proteases (data not shown). The time period of 8 h was chosen because the 25-mer substrate eluting late in the gradient is still by far the predominant peptide and the relative intensities of emerging peaks remained the same over a

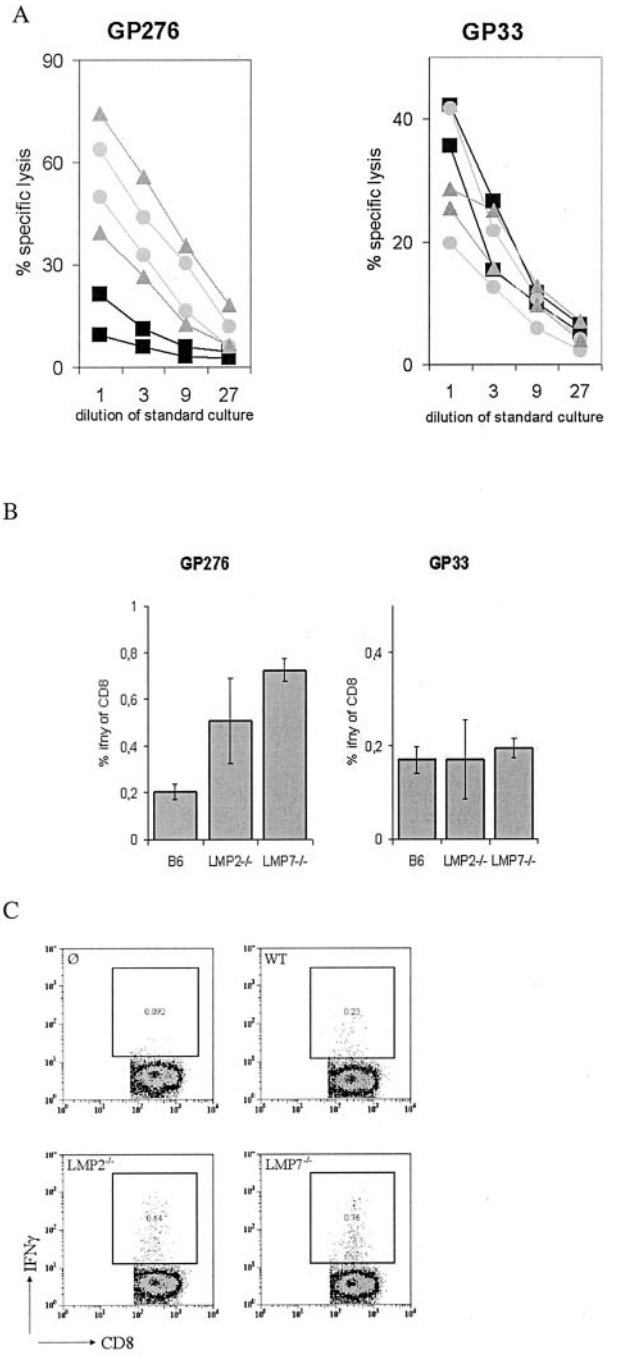

FIGURE 4. Generation of gp33–41- and gp276–286-specific CTLs in LMP2$^{-/-}$, LMP7$^{-/-}$, and C57BL/6 mice. *A*, LMP2$^{-/-}$ mice (circles), LMP7$^{-/-}$ mice (triangles), and C57BL/6 wild-type mice (squares) were infected i.p. with 2×10^6 PFU of rVVG2. Six days after infection, splenocytes were restimulated in vitro with gp33 or gp276 peptide-loaded, irradiated spleen cells. After 6 days, the restimulated spleen cells were used as effectors in a cytolytic assay. As targets, MC57 cells were used after loading with the synthetic epitopes gp276 (*left panel*) and gp33 (*right panel*). The percentage of specific lysis is plotted vs the dilution of restimulation culture. Duplicates were taken for all data points. *B*, B6, LMP2$^{-/-}$, and LMP7$^{-/-}$ mice were infected with 2×10^6 PFU of VVG2 i.p.; 7 days later, the VVG2-induced gp33–41- and gp276–286-specific CTL response was measured in the spleen by staining for CD8 and intracellular IFN-γ. Shown are the percentages of IFN-γ-positive cells of CD8$^+$ cells as determined by flow cytometry. Error bars represent SDs. The experiments have been repeated three times, yielding similar results. *C*, FACS plots of VVG2-infected C57BL/6 (wild type), LMP2$^{-/-}$, and LMP7$^{-/-}$ mice after 5-h in vitro stimulation with gp276. ∅, Represents a VVG2-infected mouse without in vitro peptide stimulation. The *y*-axis shows intracellular IFN-γ produced by CD8-positive (*x*-axis) splenocytes.

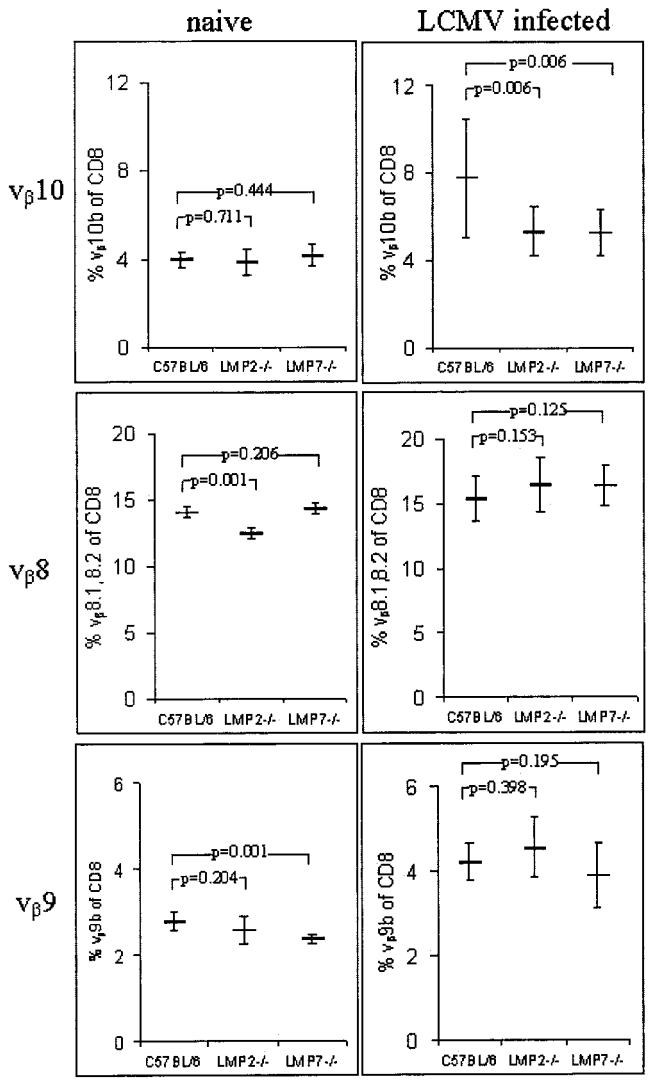

FIGURE 5. Analysis of Vβ variable segments of TCRs from C57BL/6, LMP2$^{-/-}$, and LMP7$^{-/-}$ mice. Splenocytes from naive or LCMV-infected (8 days postinfection with 200 PFU of LCMV-WE i.v.) mice were stained for CD8 and Vβ8.1/8.2, Vβ9, or Vβ10b, and analyzed by flow cytometry. Values are the means of 7 (naive) or 12 (infected) mice from two independent experiments. Values of *p* were determined by unpaired *t* test and are considered to be statistically significant when $p < 0.05$.

digestion period of up to 8 h. A further fragmentation of primary fragments was therefore unlikely to occur.

To obtain at least semiquantitative information on how the 25-mer precursor was differentially fragmented by constitutive proteasomes and immunoproteasomes, the fragments of the same digest as shown in Fig. 6*B* were analyzed by ESI-MS. A comparison of the peak intensities of ion currents from selected fragments, which could be unambiguously identified by their mass, revealed that the 11-mer epitope (residues 276–286) as well as a putative 12-mer precursor of the latter (residues 275–286) were made in greater quantity by constitutive proteasomes, whereas fragments that resulted from cleavages within the epitope (residues 280–291 and 281–289) were produced in greater amounts by immunoproteasomes (Fig. 6*C*). These data are in accordance with our Ag presentation assays, as they suggest that immunoproteasomes preferentially destroy the gp276 epitope and their precursors, whereas constitutive proteasomes are able to proteolytically generate these peptides in greater amounts.

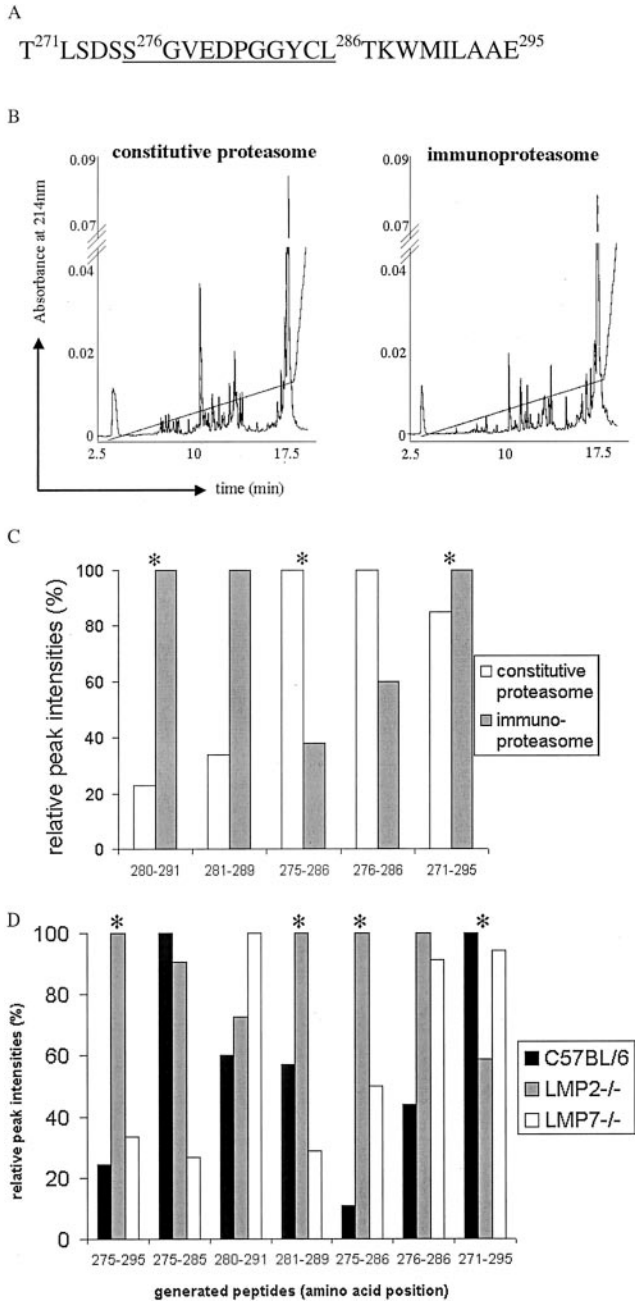

FIGURE 6. Comparison of selected fragments produced from an LCMV-gp 25-mer polypeptide by proteasome in vitro digestions. The 25-mer gp271–296 polypeptide was digested with purified 20S constitutive proteasomes and immunoproteasomes for 8 h and analyzed by HPLC-ESI-MS. *A*, Amino acid sequence of the 25-mer polypeptide containing the CTL epitope gp276–286 (underlined). *B*, Representative HPLC profiles of 25-mer polypeptide in vitro digestions (8 h) by 20S constitutive proteasome or immunoproteasome. Note that the peaks of the educt 25-mer polypeptide are of similar intensity. *C*, Comparison of selected fragments produced in the digests shown in *B*, as analyzed by HPLC-ESI-MS. The integrals of the peaks from the extracted ion chromatograms of the analyzed fragments obtained from digests by constitutive proteasomes and immunoproteasomes were compared and are shown as relative peak intensities. Peptide fragments indicated by stars represent major fragments (*D*). Comparison of selected fragments of a 25-mer (gp271–295) polypeptide in vitro digest, as analyzed by HPLC-ESI-MS with proteasome isolated from livers of LCMV-WE-infected LMP2$^{-/-}$, LMP7$^{-/-}$, and C57BL/6 mice. The integrals of the peaks from the extracted ion chromatograms of the analyzed fragments obtained from digests by proteasome isolated from livers of LCMV-WE-infected LMP2$^{-/-}$, LMP7$^{-/-}$, and C57BL/6 mice were compared and are shown as relative peak intensities. Peptide fragments indicated by stars represent major fragments.

To address the effect of LMP2 only and LMP7 only, 20S proteasome was isolated from liver of LCMV-infected LMP2- and LMP7-deficient mice. Two-dimensional gels confirmed that the two other immunoproteasome subunits were induced (data not shown). Analysis of how the 25 mer was fragmented was obtained exactly as in Fig. 6*C*. The LCMV-derived epitope gp276–286 and its putative precursor gp275–286 were produced in larger amounts by LMP2- and LMP7-deficient immunoproteasome compared with normal immunoproteasome (Fig. 6*D*), which is in accordance with the results obtained in Fig. 4, in which LMP2- and LMP7-deficient mice elicited a stronger CTL response against gp276 than wild-type mice.

Discussion

Immunodominance is an inherent and frequently observed phenomenon associated with T cell responses to viruses and other pathogens. The reason that CTLs are emerging in great numbers to only one or a few epitopes while CTLs to other potential epitopes are virtually not detectable has been profoundly investigated in the LCMV system, but the phenomenon remains poorly understood (2, 8, 9–12). Recently, it has been shown that the immunodominance of an antiviral CTL response can be shaped by the kinetics of viral protein expression (40). Nevertheless, it is still not clear why gp276 is a subdominant epitope in C57BL/6 mice after infection with LCMV. The affinity of gp276 for the peptide-binding groove of H-2D^b seems superior to that of gp33 because a ~10-fold lower concentration of gp276 was required to achieve optimal lysis (10, 11). Also, the recognition and elimination of LCMV-infected target cells by gp276-specific CTLs seem to be more efficacious compared with gp33-specific CTLs, as evidenced by adoptive transfer experiments, thus indicating that the binding of the gp276-specific TCRs to H-2D^b/gp276 complexes on the surface of LCMV-infected cells is not a limitation (11). A factor that was shown to be a determinant of immunodominance at least in influenza infection is the availability of specific CTLs in the repertoire of peripheral T cell specificities (3, 25). T cell lines specific for gp276 were strongly biased for the usage of Vα4 and Vβ10 variable segements for their TCRs (38), but it has not been investigated whether this bias imposes a limit on the availability of gp276-specific T cells in the repertoire.

Finally, gp33, gp276, and NP396 epitopes were eluted from H-2D^b proteins of LCMV-infected MC57 fibroblast cells, and the approximate number of epitopes per cell was determined. The calculated numbers were 1080 for gp33, 92 for gp276, and 162 for NP396, which implies that the copies of gp276 and NP396 epitopes generated in MC57 cells and presented on the cell surface are in a range, in which recognition by CTLs could become limiting (13, 14). However, it must be pointed out that MC57 cells infected with LCMV in vitro may not be representative for the physiological situation because infected cells in vivo are confronted with IFN-γ produced by NK cells and Th1 cells, which has dramatic effects on the class I processing and presentation pathway. In particular, we have shown that the infection of mice with LCMV, with mouse CMV, or with *Listeria monocytogenes* results in an IFN-γ-dependent and almost complete replacement of constitutive proteasomes by immunoproteasomes in the liver as well as other organs on day 7 or 8 after infection (39) (our unpublished data). We found that MC57 fibroblasts, even when they were infected with LCMV in vitro and hence produced type I IFNs, expressed mostly constitutive proteasomes (39). Moreover, not fibroblasts, but dendritic cells are the crucial APCs in the priming phase of the immune response, and these were shown to express high levels of immunoproteasomes (41, 42).

Hence, we set out to investigate immunoproteasomes as determinants of epitope hierarchy in the LCMV system. Our finding that IFN-γ treatment of MC57 cells resulted in enhanced gp33 presentation, whereas gp276 presentation was reduced (Fig. 1), inspired us to perform the experiments described in this work. An in vivo correlate to this finding has recently been reported by Rodriguez et al. (43), who showed that gp276-specific CTLs are much more prominent in IFN-γ-deficient mice, but the gp33-specific CTL response was improved in these mice as well. Another interesting phenomenon was reported by Butz and Bevan (44). They noted that when CTLs from LCMV-infected C57BL/6 mice were weekly restimulated in vitro by LCMV-infected MC57 cells, gp276-specific CTLs outgrew gp33- and NP396-specific cells within 3 wk. However, when the restimulation was performed with the dendritic cell line JawsII, gp276-specific CTLs waned, and gp33- as well as NP396-specific CTLs predominated. Given that IFN-γ stimulation leads to an almost complete replacement of constitutive proteasomes by immunoproteasomes in mouse fibroblasts within 3 days and that dendritic cells constitutively express higher amounts of immunoproteasomes than fibroblasts, we hypothesized that immunoproteasomes may be responsible for both phenomena by down-regulating gp276 peptide presentation. This hypothesis turned out to be correct, as we have shown by two independent approaches. First, we demonstrated that the overexpression of the active site subunits of immunoproteasomes LMP2, LMP7, and MECL-1 in triple transfectants caused a 2- to 4-fold down-regulation of gp276 presentation in T cell hybridoma lacZ assays (Fig. 2, *A* and *C*). Second, we showed that LCMV-infected peritoneal macrophages from LMP7$^{-/-}$ mice and to a minor extent from LMP2$^{-/-}$ were better stimulators of gp276-specific T cell hybridomas than C57BL/6 wild-type macrophages. LMP2- and LMP7-overexpressing cells indicated that mostly LMP2 is responsible for the down-regulation of gp276 in LMP2, LMP7, and MECL-1 triple transfectant (Fig. 2*C*). Comparing the fragmentation of a gp276-containing polypeptide by constitutive proteasomes and immunoproteasomes in vitro suggests that immunoproteasomes produce less gp276 precursors and destroy the gp276 epitope more frequently than constitutive proteasomes through cleavages within the epitope (Fig. 6).

Taken together, it appears that the expression of LMP2 and LMP7 negatively affects the generation of the gp276 epitope. It is, however, not possible to assign this effect to one of the subunits exclusively because their incorporation into the proteasome is to some extent interdependent. We have analyzed the subunit composition of 20S proteasomes purified from livers of LCMV-infected LMP2$^{-/-}$ and LMP7$^{-/-}$ as well as C57BL/6 wild-type mice on Coomassie-stained two-dimensional gels and found that LMP7 incorporation fully occurs in LMP2$^{-/-}$ mice in accordance with previous data (45–47). However, because the incorporation of the subunit MECL-1 barely occurs when LMP2 is missing, the effects observed in LMP2$^{-/-}$ mice could also be caused by a lack of MECL-1. In contrast, we found that the incorporation of LMP2 and MECL-1 in livers of LCMV-infected LMP7$^{-/-}$ mice occurs only to an extent of ~50%, which means that the more prominent enhancement of gp276 presentation in LMP7-deficient macrophages may at least in part be attributed to a reduction in LMP2 and MECL-1 incorporation (data not shown).

One consequence of our finding is that the number of 92 gp276 epitopes that Gallimore et al. (11) calculated to be presented by a single LCMV-infected MC57 cell will probably be much lower in cells containing immunoproteasomes, which almost completely replace constitutive proteasomes during LCMV infection in vivo. It is therefore not unexpected that the further down-regulation of gp276 epitopes by immunoproteasomes reduces gp276 epitope generation to an extent that puts a limit on the generation of gp276-specific CTLs in LCMV-infected mice. Nevertheless, the effect of immunoproteasomes on the generation of gp276-specific CTLs is not as prominent as we expected. It was not observed when LMP2$^{-/-}$ and LMP7$^{-/-}$ mice were infected with either the faster replicating WE strain or the slower replicating Armstrong strain of LCMV. However, when the mice were infected with rVVG2, which produces lower amounts of the LCMV glycoprotein, the impact of immunoproteasomes was nicely detectable (Fig. 4). We cannot rule out, however, that in addition to the effect on gp276 presentation, the greater number of gp276-specific CTLs in LMP2$^{-/-}$ and LMP7$^{-/-}$ knockout mice is due to a difference in the repertoire of peripheral T cells in these mice, as has been demonstrated for the influenza epitope NP366–374 in LMP2$^{-/-}$ mice (25). Differences in Vβ10 usage of LCMV-infected LMP2- and LMP7-deficient mice might indicate that an altered T cell repertoire of gp276-specific T cells exists in these mice (Fig. 5).

Still another interesting phenomenon observed in mice persistently infected with LCMV may be linked to our results. In two different models of chronic LCMV infection, it was recently found that the gp276 epitope that is subdominant in acute infection becomes the immunodominant epitope in chronically infected mice, whereas gp33 and NP396 drop deeply in epitope hierarchy (48, 49). Both research groups report that in chronic infection, the LCMV-specific CTLs stop to produce TNF-α and IFN-γ, which are the cardinal inducers of immunoproteasomes. We propose that this reversion in epitope hierarchy is at least in part due to a drop in the cellular content of immunoproteasomes.

Acknowledgments

We thank Dr. Tomoki Chiba and Dr. John Monaco for the contribution of mice, and Katrin Schwarz for the performance of some initial experiments. Dr. Cornelia Kolb is acknowledged for supplying purified proteasomes, and Dr. Frank Momburg for providing the H-2D^b expression construct. We are grateful to Eugene N. Damoc for help with mass spectroscopy.

References

1. Deng, Y., J. W. Yewdell, L. C. Eisenlohr, and J. R. Bennink. 1997. MHC affinity, peptide liberation, T cell repertoire, and immunodominance all contribute to the paucity of MHC class I-restricted peptides recognized by antiviral CTL. *J. Immunol. 158:1507.*
2. Gallimore, A., J. Hombach, T. Dumrese, H. G. Rammensee, R. M. Zinkernagel, and H. Hengartner. 1998. A protective cytotoxic T cell response to a subdominant epitope is influenced by the stability of the MHC class I/peptide complex and the overall spectrum of viral peptides generated within infected cells. *Eur. J. Immunol. 28:3301.*
3. Chen, W., L. C. Anton, J. R. Bennink, and J. W. Yewdell. 2000. Dissecting the multifactorial causes of immunodominance in class I-restricted T cell responses to viruses. *Immunity 12:83.*
4. Yewdell, J. T., and J. R. Bennink. 1999. Immunodominance in major histocompatibility complex class I-restricted T lymphocyte responses. *Annu. Rev. Immunol. 17:51.*
5. Townsend, A., J. Bastin, K. Gould, G. Brownlee, M. Andrew, B. Coupar, D. Boyle, S. Chan, and G. Smith. 1988. Defective presentation to class I-restricted cytotoxic T lymphocytes in vaccinia-infected cells is overcome by enhanced degradation of antigen. *J. Exp. Med. 168:1211.*
6. Rammensee, H. G., J. Bachmann, N. P. N. Emmerich, O. A. Bachor, and S. Stevanovic. 1999. SYFPEITHI: database for MHC ligands and peptide motifs. *Immunogenetics 50:213.*
7. Lanzavecchia, A., G. Iezzi, and A. Viola. 1999. From TCR engagement to T cell activation: a kinetic view of T cell behavior. *Cell 96:1.*
8. Slifka, M. K., J. N. Blattman, D. J. Sourdive, F. Liu, D. L. Huffman, T. Wolfe, A. Hughes, M. B. Oldstone, R. Ahmed, and M. G. Von Herrath. 2003. Preferential escape of subdominant CD8$^+$ T cells during negative selection results in an altered antiviral T cell hierarchy. *J. Immunol. 170:1231.*
9. Van der Most, R. G., A. Sette, C. Oseroff, J. Alexander, K. Murali-Krishna, L. L. Lau, S. Southwood, J. Sidney, R. W. Chestnut, M. Matloubian, and R. Ahmed. 1996. Analysis of cytotoxic T cell responses to dominant and subdominant epitopes during acute and chronic lymphocytic choriomeningitis virus infection. *J. Immunol. 157:5543.*
10. Van der Most, R. G., K. MuraliKrishna, J. L. Whitton, C. Oseroff, J. Alexander, S. Southwood, J. Sidney, R. W. Chesnut, A. Sette, and R. Ahmed. 1998. Identification of D-b- and K-b-restricted subdominant cytotoxic T- cell responses in lymphocytic choriomeningitis virus-infected mice. *Virology 240:158.*

11. Gallimore, A., T. Dumrese, H. Hengartner, R. M. Zinkernagel, and H.-G. Rammensee. 1998. Protective immunity does not correlate with the hierarchy of virus-specific cytotoxic T cell responses to naturally processed peptides. *J. Exp. Med. 187:1647*.
12. Weidt, G., O. Utermohlen, J. Heukeshoven, F. Lehmann-Grube, and W. Deppert. 1998. Relationship among immunodominance of single $CD8^+$ T cell epitopes, virus load, and kinetics of primary antiviral CTL response. *J. Immunol. 160:2923*.
13. Christinck, E. R., M. A. Luscher, B. H. Barber, and D. B. Williams. 1991. Peptide binding to class I MHC on living cells and quantitation of complexes required for CTL lysis. *Nature 352:67*.
14. Kageyama, S., T. J. Tsomides, Y. Sykulev, and H. N. Eisen. 1995. Variations in the number of peptide-MHC class I complexes required to activate cytotoxic T cell responses. *J. Immunol. 154:567*.
15. Schwarz, K., R. de Giuli, G. Schmidtke, S. Kostka, M. van den Broek, K. Kim, C. M. Crews, R. Kraft, and M. Groettrup. 2000. The selective proteasome inhibitors lactacystin and expoxomicin can be used to either up- or down-regulate antigen presentation at non-toxic doses. *J. Immunol. 164:6147*.
16. Groettrup, M., A. Soza, U. Kuckelkorn, and P. M. Kloetzel. 1996. Peptide antigen production by the proteasome: complexity provides efficiency. *Immunol. Today 17:429*.
17. Voges, D., P. Zwickl, and W. Baumeister. 1999. The 26S proteasome: a molecular machine designed for controlled proteolysis. *Annu. Rev. Biochem. 68:1015*.
18. Gileadi, U., H. T. MoinsTeisserenc, I. Correa, B. L. Booth, P. R. Dunbar, A. K. Sewell, J. Trowsdale, R. E. Phillips, and V. Cerundolo. 1999. Generation of an immunodominant CTL epitope is affected by proteasome subunit composition and stability of the antigenic protein. *J. Immunol. 163:6045*.
19. Schwarz, K., M. van den Broek, S. Kostka, R. Kraft, A. Soza, G. Schmidtke, P. M. Kloetzel, and M. Groettrup. 2000. Overexpression of the proteasome subunits LMP2, LMP7, and MECL-1 but not PA28α/β enhances the presentation of an immunodominant lymphocytic choriomeningitis virus T cell epitope. *J. Immunol. 165:768*.
20. Sijts, A. J. A. M., S. Standera, R. E. M. Toes, T. Ruppert, N. J. C. M. Beekman, P. A. vanVeelen, F. A. Ossendorp, C. J. M. Melief, and P. M. Kloetzel. 2000. MHC class I antigen processing of an adenovirus CTL epitope is linked to the levels of immunoproteasomes in infected cells. *J. Immunol. 164:4500*.
21. Schultz, E. S., J. Chapiro, C. Lurquin, S. Claverol, O. BurletSchiltz, G. Warnier, V. Russo, S. Morel, F. Levy, T. Boon, et al. 2002. The production of a new MAGE-3 peptide presented to cytolytic T lymphocytes by HLA-B40 requires the immunoproteasome. *J. Exp. Med. 195:391*.
22. Morel, S., F. Levy, O. BurletSchiltz, F. Brasseur, M. ProbstKepper, A. L. Peitrequin, B. Monsarrat, R. VanVelthoven, J. C. Cerottini, T. Boon, et al. 2000. Processing of some antigens by the standard proteasome but not by the immunoproteasome results in poor presentation by dendritic cells. *Immunity 12:107*.
23. Van Kaer, L., P. G. Ashton-Rickardt, M. Eichelberger, M. Gaczynska, K. Nagashima, K. L. Rock, A. L. Goldberg, P. C. Doherty, and S. Tonegawa. 1994. Altered peptidase and viral-specific T cell response in LMP 2 mutant mice. *Immunity 1:533*.
24. Fehling, H. J., W. Swat, C. Laplace, R. Kuehn, K. Rajewsky, U. Mueller, and H. von Boehmer. 1994. MHC class I expression in mice lacking proteasome subunit LMP-7. *Science 265:1234*.
25. Chen, W. S., C. C. Norbury, Y. J. Cho, J. W. Yewdell, and J. R. Bennink. 2001. Immunoproteasomes shape immunodominance hierarchies of antiviral $CD8^+$ T cells at the levels of T cell repertoire and presentation of viral antigens. *J. Exp. Med. 193:1319*.
26. Dubiel, W., G. Pratt, K. Ferrell, and M. Rechsteiner. 1992. Purification of an 11S regulator of the multicatalytic proteinase. *J. Biol. Chem. 267:22369*.
27. Chu-Ping, M., C. A. Slaughter, and G. N. DeMartino. 1992. Identification, purification and characterization of a protein activator (PA28) of the 20S proteasome (macropain). *J. Biol. Chem. 267:10515*.
28. Groettrup, M., T. Ruppert, L. Kuehn, M. Seeger, S. Standera, U. Koszinowski, and P. M. Kloetzel. 1995. The interferon-γ-inducible 11S regulator (PA28) and the LMP2/LMP7 subunits govern the peptide production by the 20S proteasome in vitro. *J. Biol. Chem. 270:23808*.
29. Groettrup, M., A. Soza, M. Eggers, L. Kuehn, T. P. Dick, H. Schild, H.-G. Rammensee, U. H. Koszinowski, and P.-M. Kloetzel. 1996. A role for the proteasome regulator PA28α in antigen presentation. *Nature 381:166*.
30. Schwarz, K., M. Eggers, A. Soza, U. H. Koszinowski, P. M. Kloetzel, and M. Groettrup. 2000. The proteasome regulator PA28α/β can enhance antigen presentation without affecting 20S proteasome subunit composition. *Eur. J. Immunol. 30:3672*.
31. Van Hall, T., A. Sijts, M. Camps, R. Offringa, C. Melief, P. M. Kloetzel, and F. Ossendorp. 2000. Differential influence on cytotoxic T lymphocyte epitope presentation by controlled expression of either proteasome immunosubunits or PA28. *J. Exp. Med. 192:483*.
32. Yamano, T., S. Murata, N. Shimbara, N. Tanaka, T. Chiba, K. Tanaka, K. Yui, and H. Udono. 2002. Two distinct pathways mediated by PA28 and hsp90 in major histocompatibility complex class I antigen processing. *J. Exp. Med. 196:185*.
33. Preckel, T., W. Fung-Leung, Z. Cai, A. Vitiello, L. Salter-Cid, O. Winqvist, T. G. Wolfe, M. von Herrath, A. Angulo, P. Ghazal, et al. 1999. Impaired immunoproteasome assembly and immune responses in $PA28^{-/-}$ mice. *Science 286:2162*.
34. Murata, S., H. Udono, N. Tanahashi, N. Hamada, K. Watanabe, K. Adachi, T. Yamano, K. Yui, N. Kobayashi, M. Kasahara, et al. 2001. Immunoproteasome assembly and antigen presentation in mice lacking both PA28α and PA28β. *EMBO J. 20:5898*.
35. Aden, D. P., and B. B. Knowles. 1976. Cell surface antigens coded for by the human chromosome 7. *Immunogenetics 3:209*.
36. Bruns, M., J. Cihak, G. Müller, and F. Lehmann-Grube. 1983. Lymphocytic choriomeningitis virus. VI. Isolation of a glycoprotein mediating neutralization. *Virology 130:247*.
37. Schwarz, K., M. van den Broek, R. de Giuli, W. W. Seelentag, N. Shastri, and M. Groettrup. 2000. The use of LCMV-specific Tcell hybridomas for the quantitative analysis of MHC class I restricted antigen presentation. *J. Immunol. Methods 237:199*.
38. Aebischer, T., S. Oehen, and H. Hengartner. 1990. Preferential usage of Vα4 and Vβ10 T cell receptor genes by lymphocytic choriomeningitis virus glycoprotein-specific $H\text{-}2D^b$-restricted cytotoxic T cells. *Eur. J. Immunol. 20:523*.
39. Khan, S., M. van den Broek, K. Schwarz, R. de Giuli, P. A. Diener, and M. Groettrup. 2001. Immunoproteasomes largely replace constitutive proteasomes during an antiviral and antibacterial immune response in the liver. *J. Immunol. 167:6859*.
40. Probst, H. C., K. Tschannen, A. Gallimore, M. Martinic, M. Basler, T. Dumrese, E. Jones, and M. F. van den Broek. 2003. Immunodominance of an antiviral cytotoxic T cell response is shaped by the kinetics of viral protein expression. *J. Immunol. 171:5415*.
41. Macagno, A., M. Gilliet, F. Sallusto, A. Lanzavecchia, F. O. Nestle, and M. Groettrup. 1999. Dendritic cells up-regulate immunoproteasomes and the proteasome regulator PA28 during maturation. *Eur. J. Immunol. 29:4037*.
42. Macagno, A., L. Kuehn, R. de Giuli, and M. Groettrup. 2001. Pronounced up-regulation of the PA28α/β proteasome regulator but little increase in the steady state content of immunoproteasomes during dendritic cell maturation. *Eur. J. Immunol. 31:3271*.
43. Rodriguez, F., S. Harkins, M. K. Slifka, and J. L. Whitton. 2002. Immunodominance in virus-induced $CD8^+$ T-cell responses is dramatically modified by DNA immunization and is regulated by γ interferon. *J. Virol. 76:4251*.
44. Butz, E. A., and M. J. Bevan. 1998. Differential presentation of the same MHC class I epitopes by fibroblasts and dendritic cells. *J. Immunol. 160:2139*.
45. Groettrup, M., S. Standera, R. Stohwasser, and P. M. Kloetzel. 1997. The subunits MECL-1 and LMP2 are mutually required for incorporation into the 20S proteasome. *Proc. Natl. Acad. Sci. USA 94:8970*.
46. Griffin, T. A., D. Nandi, M. Cruz, H. J. Fehling, L. VanKaer, J. J. Monaco, and R. A. Colbert. 1998. Immunoproteasome assembly: cooperative incorporation of interferon γ (IFN-γ)-inducible subunits. *J. Exp. Med. 187:97*.
47. De, M., K. Jayarapu, L. Elenich, J. J. Monaco, R. A. Colbert, and T. A. Griffin. 2003. β2 subunit propeptides influence cooperative proteasome assembly. *J. Biol. Chem. 278:6153*.
48. Wherry, E. J., J. N. Blattman, K. Murali-Krishna, R. van der Most, and R. Ahmed. 2003. Viral persistence alters CD8 T-cell immunodominance and tissue distribution and results in distinct stages of functional impairment. *J. Virol. 77:4911*.
49. Fuller, M. J., and A. J. Zajac. 2003. Ablation of CD8 and CD4 T cell responses by high viral loads. *J. Immunol. 170:477*.